

# CD22 $\Delta$ E12 as a molecular target for RNAi therapy

Fatih M. Uckun,<sup>1,2,3</sup> Hong Ma,<sup>1</sup> Jianjun Cheng,<sup>4</sup> Dorothea E. Myers<sup>1</sup> and Sanjive Qazi<sup>1,5</sup>

<sup>1</sup>Children's Center for Cancer and Blood Diseases, Children's Hospital Los Angeles (CHLA), <sup>2</sup>Division of Hematology-Oncology, Department of Pediatrics, University of Southern California Keck School of Medicine (USC KSOM), <sup>3</sup>Translational and Clinical Sciences Program, Norris Comprehensive Cancer Center, University of Southern California Keck School of Medicine (USC KSOM), Los Angeles, CA, <sup>4</sup>Department of Materials Science and Engineering, University of Illinois at Urbana-Champaign, Urbana, IL, and <sup>5</sup>Bioinformatics Program, Gustavus Adolphus College, St. Peter, MN, USA

Received 26 October 2014; accepted for publication 3 December 2014

Correspondence: Fatih M. Uckun, 4650 Sunset Boulevard, Smith Research Tower Suite 300-316, Children's Center for Cancer and Blood Diseases, CHLA Mailstop 160, Los Angeles, CA 90027.

E-mail: fmuckun@chla.usc.edu

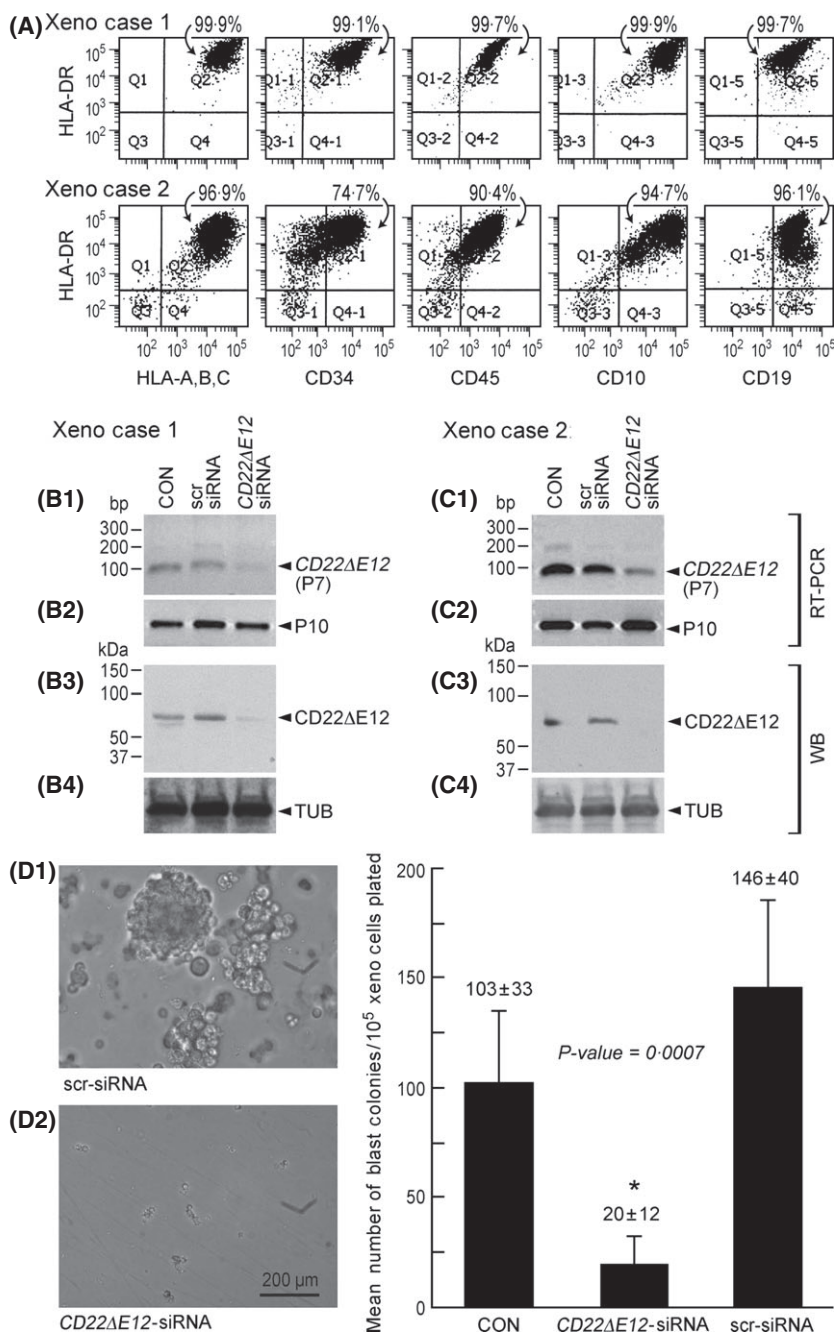
## Summary

B-precursor acute lymphoblastic leukaemia (BPL) is the most common form of cancer in children and adolescents. Our recent studies have demonstrated that CD22 $\Delta$ E12 is a characteristic genetic defect of therapy-refractory clones in paediatric BPL and implicated the CD22 $\Delta$ E12 genetic defect in the aggressive biology of relapsed or therapy-refractory paediatric BPL. The purpose of the present study is to evaluate the biological significance of the CD22 $\Delta$ E12 molecular lesion in BPL and determine if it could serve as a molecular target for RNA interference (RNAi) therapy. Here we report a previously unrecognized causal link between CD22 $\Delta$ E12 and aggressive biology of human BPL cells by demonstrating that siRNA-mediated knockdown of CD22 $\Delta$ E12 in primary leukaemic B-cell precursors is associated with a marked inhibition of their clonogenicity. Additionally, we report a nanoscale liposomal formulation of CD22 $\Delta$ E12-specific siRNA with potent *in vitro* and *in vivo* anti-leukaemic activity against primary human BPL cells as a first-in-class RNAi therapeutic candidate targeting CD22 $\Delta$ E12.

**Keywords:** acute leukaemia, molecular pathogenesis, new drugs for leukaemia, childhood haematological malignancies, experimental therapies.

CD22, a member of the Siglec (sialic acid-binding Ig-like lectins) family of regulators of the immune system, is a negative regulator of multiple signal transduction pathways critical for proliferation and survival of B-lineage lymphoid cells. The inhibitory and apoptosis-promoting signalling functions of CD22 are dependent on recruitment of the Src homology 2 domain-containing inhibitory tyrosine phosphatase (SHP)-1 to the immunoreceptor tyrosine-based inhibitory motifs (ITIMs) of its cytoplasmic domain upon phosphorylation by the Src family tyrosine kinase LYN. Without the inhibitory function of CD22, signalling pathways in B-lineage lymphoid cells would remain in 'overdrive', contributing to abnormal proliferation. B-precursor acute lymphoblastic leukaemia (BPL) is the most common form of cancer in children and adolescents. BPL cells express a dysfunctional CD22 due to deletion of Exon 12 (CD22 $\Delta$ E12) arising from a splicing defect associated with homozygous intronic mutations (Uckun *et al*, 2010a). CD22 $\Delta$ E12 results in a truncating frame shift mutation yielding a mutant CD22 $\Delta$ E12 protein that lacks most of the intracellular domain including the key regulatory signal trans-

duction elements, such as the ITIMs that provide docking sites for the SH2 domains of SHP1, and all of the cytoplasmic tyrosine residues (Uckun *et al*, 2010a). Our recent studies have demonstrated that CD22 $\Delta$ E12 is a characteristic genetic defect of therapy-refractory clones in paediatric BPL and implicated the CD22 $\Delta$ E12 genetic defect in the aggressive biology of relapsed or therapy-refractory paediatric BPL (Ma *et al*, 2012). The purpose of the present study is to evaluate the biological significance of the CD22 $\Delta$ E12 molecular lesion in BPL and determine if it can serve as a molecular target for RNA interference (RNAi) therapy. Here we report a previously unrecognized causal link between CD22 $\Delta$ E12 and aggressive biology of BPL cells by demonstrating that siRNA-mediated knockdown of CD22 $\Delta$ E12 in primary BPL cells is associated with a marked inhibition of their clonogenicity. Systemically administered unformulated siRNA lack RNAi activity *in vivo* due to rapid enzymatic degradation in blood and very poor entry into target cells. There is an urgent and unmet need to identify delivery systems capable of safely and efficiently delivering siRNA to molecular targets not amenable to other drug-delivery



approaches. Several investigators have reported preclinical and early clinical proof-of-concept studies demonstrating that systemic delivery of an siRNA nanoparticle targeting a specific gene transcript can elicit biological responses *in vivo* (Uckun & Yiv, 2012; Wang, 2014). As nanoparticles can protect siRNA from degradation, facilitate their cellular uptake by endocytosis and enable an effective RNAi by allowing the endosomal escape of the endocytosed siRNA into the cytoplasm, they are generally considered the most appropriate dosage forms for siRNA as a new class of therapeutic agents against otherwise undruggable molecular targets (Wang, 2014). We report a nanoscale liposomal formulation of CD22ΔE12-specific siRNA

with promising *in vitro* and *in vivo* anti-leukaemic activities against primary human BPL cells as an RNAi therapeutic candidate targeting CD22ΔE12. These results establish the CD22ΔE12 oncoprotein as a molecular target for effective RNAi therapy against BPL.

## Materials and methods

### Leukaemia cells

We used 6 acute lymphoblastic leukaemia (ALL) xenograft clones that were derived from spleen specimens of xenografted

**Fig 1.** RNAi Knockdown of *CD22ΔE12* in Aggressive Human BPL Xenograft Cells. (A) Depicted are representative fluorescence-activated cell sorting (FACS)-correlated two-parameter displays of B-precursor acute lymphoblastic leukaemia (BPL) xenograft cells isolated from spleens of NOD/SCID mice that developed overt leukaemia after inoculation with primary ALL cells from BPL patients. Cells were stained by direct immunofluorescence for human lymphoid differentiation antigens CD10, CD19, CD34, CD45, HLA-DR/DP/DQ, and HLA-A,B,C. The labelled cells were analysed on a LSR II flow cytometer. Xenograft cells co-expressed CD45, HLA-DR/DP/DQ and HLA-A,B,C antigens and had an immature B-cell precursor immunophenotype characterized by co-expression of B-lineage progenitor antigens CD10/CALLA, CD19, and CD34. (B & C) Cells were transfected with a Nucleofector II device (Amaxa GmbH, Basel, Switzerland; protocol VCA-1002/C005) with either *CD22ΔE12*-siRNA (50 nmol/l) or scr-siRNA (50 nmol/l). Controls included untreated cells. Depicted in B1 and C1 are images of 1% agarose gels showing the reverse transcription polymerase chain reaction (RT-PCR) products obtained from the RNA samples of *CD22ΔE12*-siRNA transfected xenograft cells using the P7 primer pair to amplify a 182-bp region (c.2180–c.2361) of the *CD22* cDNA extending from Exon 11 to Exon 13 and spanning the entire Exon 12. Deletion of Exon 12 results in a smaller *CD22ΔE12*-specific PCR product of 63-bp size with this primer set migrating slightly below the 100-bp size marker. The P10 primer set was used as a positive control of RNA integrity to amplify a 213-bp region (c.433–c.645) of the *CD22* cDNA present in both wildtype *CD22* and *CD22ΔE12* mRNA species (B2, C2). The 63-bp *CD22ΔE12*-mRNA was abundant in the total RNA isolated from the BPL xenograft clones. RT-PCR products were sized using the 1 Kb Plus DNA ladder from Invitrogen/Life Technologies (Grand Island, NY, USA). Gel images were taken with an UVP digital camera and UV light in an Epi Chemi II Darkroom using the LabWorks Analysis software (UVP, Upland, CA). Whole cell lysates of xenograft cells were subjected to CD22 and alpha-Tubulin (TUB) Western blot (WB) analysis. The positions of truncated mutant *CD22ΔE12* protein (B3, C3) and TUB (B4, C4) are indicated with arrowheads. BPL xenograft cells expressed a *CD22ΔE12*-associated truncated CD22 protein instead of the 130/140-kDa intact CD22 protein. Transfection with *CD22ΔE12*-siRNA, but not scrambled (scr)-siRNA, caused selective depletion of *CD22ΔE12*-mRNA as well as *CD22ΔE12*-protein in aggressive BPL xenograft cells. (D, E) We evaluated the effects of *CD22ΔE12*-siRNA versus scr-siRNA (50 nmol/l) on blast colony formation in day 7 methylcellulose (0.9%) cultures of xenograft cells derived from 6 BPL patients (3 newly diagnosed – including one patient with Ph<sup>+</sup> BPL- and three relapsed paediatric BPL patients). Colony formation was examined using an inverted Nikon Eclipse TS100 microscope (Nikon, Melville, NY, USA). Images were taken using a Digital Sight DS-2MBW Nikon camera. Depicted in D1 is the image of a representative blast colony and 2 adjacent blast clusters in day 7 cultures of scr-siRNA transfected xenograft cells from a representative case. No blast colonies or clusters were observed in cultures of *CD22ΔE12*-siRNA transfected cells in this particular case (D2). The bar graphs shown in E depict the mean ± SE values for blast colonies per 100 000 cells plated for all ALL xenograft clones ( $n = 6$ ). The mean (±SE) numbers of blast colonies per 100 000 cells plated were  $103 \pm 33$  in untreated controls,  $146 \pm 40$  after scr-siRNA transfection, and only  $20 \pm 12$  after *CD22ΔE12*-siRNA transfection (Linear contrast  $P$ -value = 0.0007). \*Difference from CON statistically significant

non-obese diabetic-severe combined immunodeficiency (NOD/SCID) mice inoculated with leukaemia cells from three newly diagnosed (including one patient with Ph<sup>+</sup> BPL) and three relapsed paediatric BPL patients. The secondary use of leukaemic cells for subsequent laboratory studies did not meet the definition of human subject research per 45 CFR 46.102 (d and f) because it did not include identifiable private information, and it was approved by the Institutional Review Board (IRB) (Committee on Clinical Investigations, CCI) at the Children's Hospital Los Angeles (CHLA) (CCI-10-00141; CCI Review Date: 7-27-2010; IRB Approval: 7-27-2010). Human Subject Assurance Number: FWA0001914. We also used the ALL-1 (Ph<sup>+</sup> adult BPL) and RAJI (Burkitt leukaemia/B-cell ALL) cell lines. RAJI is a radiation-resistant Burkitt leukaemia/B-ALL cell line. ALL-1 is a chemotherapy-resistant BCR-ABL1<sup>+</sup> t(9; 22)/Ph<sup>+</sup> pre-pre-B ALL cell line. Both cell lines are *CD22ΔE12*-positive and have homozygous intronic *CD22* gene mutations at Rs10413526 (C>G) and Rs4805120 (A>G) that are associated with *CD22ΔE12* (Uckun *et al*, 2010a; Ma *et al*, 2012). Both cell lines, as well as each of the 6 ALL xenograft clones, were confirmed to be *CD22ΔE12*<sup>+</sup> using a quantitative reverse transcription polymerase chain reaction (RT-PCR) assay (Uckun *et al*, 2014). The PCR primer pair was designed to amplify a 113-bp fragment spanning from Exon 11 to Exon 13 of the human *CD22* cDNA. The amplified fragment was then specifically annealed to a pre-mixed oligo DNA probe (5'-TGTGAG-GAATAAAAAGAGATGCAGAGTCC-3') conjugated with 5'

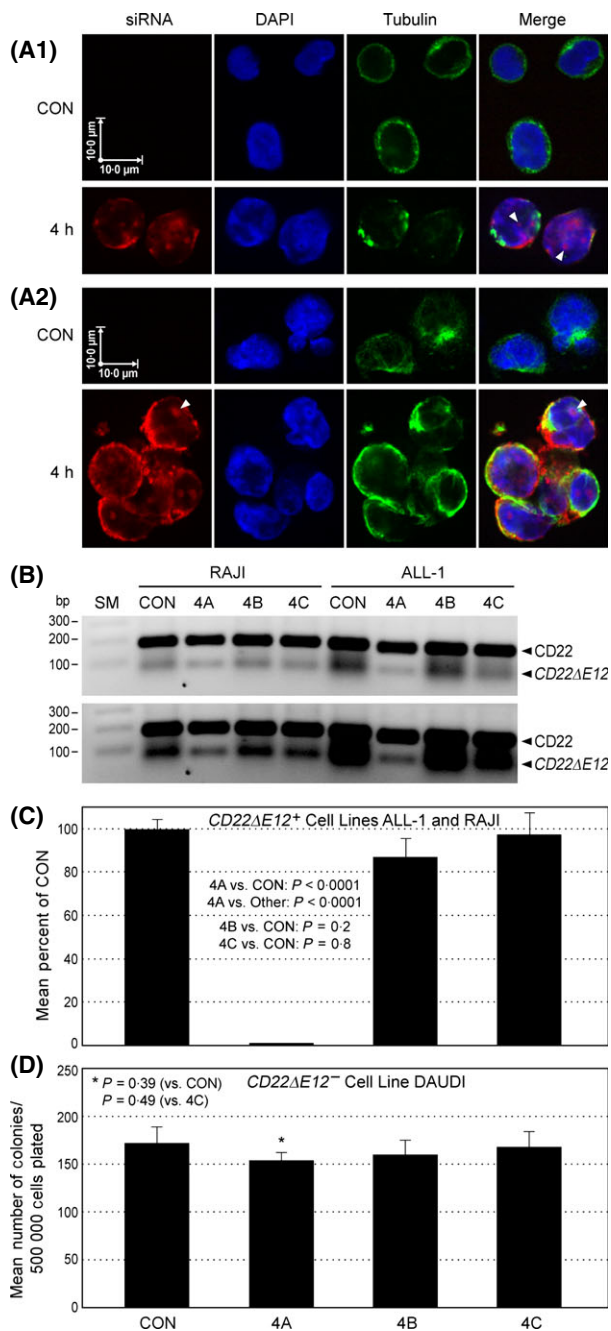
FAM reporter and 3'BHQ Quencher on the *CD22ΔE12*-specific unique junction region between Exon 11 and Exon 13. A normalization procedure employing *ACTB* RT-PCR results was utilized to calculate the delta ( $\Delta$ )Ct values. The  $\Delta\Delta$ Ct values were determined by subtracting the mean  $\Delta$ Ct value for negative controls (*viz.*, 293-T human kidney cell line; mean delta Ct =  $18.7 \pm 1.6$ ) from the  $\Delta$ Ct values for each sample. See Supporting Information for a more detailed description. The  $\Delta$ Ct/ $\Delta\Delta$ Ct values were 6.2/–12.5 for RAJI cells and 8.7/–10.0 for ALL-1 cells. The  $\Delta$ Ct/ $\Delta\Delta$ Ct values for the 6 xenograft clones were 12.8/–5.9, 14.4/–4.3, 9.7/–9.0, 8.3/–10.4, 13.4/–5.3 and 12.9/–5.8, respectively.

#### Transfections and PCR assays

Transfections of ALL cells with small interfering RNA (siRNA) were accomplished using standard methods and procedures. PCR and RT-PCR assays were also performed according to standard procedures. See Supporting Information for a more detailed description of these methodologies.

#### In vitro assays

We used standard assays and procedures, including Western blot assays, RT-PCR, colony assays, flow cytometric apoptosis assays, immunophenotyping, confocal imaging, and genomic PCR. See Supporting Information for a more detailed description of these methodologies (Uckun *et al*, 2010b, 2011, 2012).



### Preparation of a nanoscale liposomal CD22ΔE12-siRNA formulation

We prepared a liposomal nanoformulation (LNF) of the CD22ΔE12-siRNA duplex using the standard thin film evaporation method and used standard methods to characterize it (Uckun *et al*, 2013; Myers *et al*, 2014). See Supporting Information for a more detailed description of these methodologies.

### Transgenic (Tg) mice

Pronuclear microinjection of the human CD22ΔE12 transgene (European Nucleotide Archive [ENA], Acces-

Fig 2. Cellular Uptake, RNAi Activity and Cytotoxicity of CD22ΔE12-siRNA liposomal nanoformulation (LNF). (A). We used 5' Cy3-labelled CD22ΔE12-siRNA to prepare the LNF of CD22ΔE12-siRNA for cellular uptake and trafficking experiments using confocal imaging. Depicted are confocal images demonstrating the LNF-mediated CD22ΔE12-siRNA delivery into the BCR-ABL1<sup>+</sup> human BPL cell line ALL-1 (depicted in A1) and the Burkitt leukaemia cell line RAJI (depicted in A2). After incubation with the LNF of Cy3-labelled siRNA (49.5 nmol/l) for 1, 2, or 4 h, the internalized Cy3-labelled CD22ΔE12-siRNA was detected and localized using the tetramethyl rhodamine (TRITC) filter sets. Cells were also stained with an anti-alpha-Tubulin MoAb and subsequently incubated with green-fluorescent Alexa Fluor 488 dye-labelled goat anti-mouse IgG (secondary Ab). Cells were then washed with phosphate-buffered saline and counterstained with the blue fluorescent DNA-specific nuclear dye 4',6-diamidino-2-phenylindole (DAPI). Slides were imaged using the PerkinElmer Spinning Disc Confocal Microscope and the PerkinElmer UltraView ERS software (Shelton, CT) or the Velocity V5.4 imaging software (PerkinElmer, Shelton, CT). Depicted are representative images of cells incubated with the CD22ΔE12-siRNA LNF for 4 h. Similar results were obtained after 1-h and 2 h incubations as well as after a 1-h treatment with the LNF, wash and 24-h incubation in the absence of the LNF. Arrowheads point to location of Cy3-labelled siRNA molecules inside the DAPI-stained (blue) nucleus and tubulin-containing (green) perinuclear cytoplasm. (B) Depicted are images of a 1% agarose gel showing the RT-PCR products obtained from the RNA samples of CD22ΔE12-siRNA LNF-treated ALL-1 and RAJI cells using the P7 primer pair to amplify a 182-bp region (c.2180–c.2361) of the CD22 cDNA extending from Exon 11 to Exon 13 and spanning the entire Exon 12. RT-PCR products were sized using the 1 Kb Plus DNA ladder from Invitrogen/Life Technologies. Deletion of Exon 12 results in a smaller CD22ΔE12-specific PCR product of 63-bp size with this primer set. Gel images were taken with an UVP digital camera and UV light in the Epi Chemi II Darkroom using the LabWorks Analysis software (UVP, Upland, CA). Cells were treated for 48 h with the CD22ΔE12-siRNA LNF 4A (49.5 nmol/l siRNA, 117 μmol/l lipid), the scrambled-siRNA containing LNF 4C (90.6 nmol/l siRNA, 117 μmol/l lipid) or the siRNA-free LNF 4B (0 nmol/l siRNA, 117 μmol/l lipid). (C & D) Effects of CD22ΔE12 depletion by 4A on the *in vitro* clonogenicity of the CD22ΔE12<sup>+</sup> human leukaemia cell lines ALL-1 and RAJI (combined dataset depicted in C) versus the CD22ΔE12<sup>-</sup> human leukaemia/lymphoma cell line DAUDI (depicted in D). Concentrations of formulations used were: 4A treatment: 49.5 nmol/l siRNA, 117 μmol/l lipid; 4B treatment: 0 nmol/l siRNA, 117 μmol/l lipid; 4C treatment: 90.6 nmol/l scrambled siRNA, 117 μmol/l lipid. Untreated cells (CON) as well as cells ( $0.5 \times 10^5$  cells/plate, in duplicate) treated with CD22ΔE12-siRNA formulation 4A or control formulations 4B and 4C were examined for colony formation in methylcellulose supplemented (0.9%) cultures. Colony formation was examined using an inverted Nikon Eclipse TS100 microscope. Treatment with 4A (but not control formulations 4B or 4C) abrogated leukaemic cell clonogenicity. Depicted are bar graphs of mean (% of untreated control/CON) colony formation for ALL-1 and RAJI cells after treatment with 4A versus control LNF 4B or 4C. The day 7 colony counts in untreated control cultures were  $333 \pm 19$  colonies/ $0.5 \times 10^5$  cells for ALL-1 cells and  $72 \pm 3$  colonies/ $0.5 \times 10^5$  cells for RAJI cells. No colonies were detected in cultures of 4A-treated ALL-1 or RAJI cells. By comparison, there were  $336 \pm 20$  colonies/ $0.5 \times 10^5$  ALL-1 cells and  $53 \pm 3$  colonies/ $0.5 \times 10^5$  RAJI cells, respectively, in cultures of 4B-treated cells. Likewise, there were  $353 \pm 65$  colonies/ $0.5 \times 10^5$  ALL-1 cells and  $64 \pm 5$  colonies/ $0.5 \times 10^5$  RAJI cells, respectively, in cultures of 4C-treated cells. The values for mean % of control colony formation were not significantly reduced for 4B- ( $87.2 \pm 8.4\%$ ,  $P = 0.2$ ) or 4C-treated cells ( $97.8 \pm 9.7\%$ ,  $P = 0.8$ ). Colony formation by the DAUDI cell line was not affected by CD22ΔE12-siRNA LNF. Depicted in (D) are the mean numbers of colonies per  $5 \times 10^5$  cells for DAUDI cells after various treatments. \*Difference from CON not statistically significant

sion#LM652705), founder generation, and genotyping analysis of tail DNA, PCR-based clonality assays (ENA, Accession # LM652707), immunophenotyping by multi-parameter flow cytometry, Western blot analyses, fluorescent *in situ* hybridization (FISH) and spectral karyotyping (SKY) were performed using standard methods. See Supporting Information for a more detailed description of these methodologies.

#### *NOD/SCID mouse xenograft model of human BPL*

The anti-leukaemic activity of CD22ΔE12-siRNA LNF was studied in a NOD/SCID mouse model of human BPL.

#### *Pharmacokinetic (PK) Studies*

The research was conducted according to Institutional Animal Care and Use Committee (IACUC) Protocols that were approved by the IACUC of CHLA. We first used the CD22ΔE12-siRNA LNF prepared using the Cy3-labelled CD22ΔE12-siRNA as a PK formulation in PK experiments. The Cy3-based fluorescence of the plasma samples was determined at emission wavelength of 590 nm (530 nm excitation wavelength) using the Synergy HT Biotek fluorescence microplate reader and the Gen5 software (BioTek Instruments Inc., Winooski, VT, USA). For validation employing a different assay platform, we used a quantitative RT-PCR technique and measured CD22ΔE12-specific siRNA levels in plasma samples after administration of CD22ΔE12-siRNA LNF prepared with unlabelled CD22ΔE12-siRNA. Pharmacokinetic modelling and pharmacokinetic parameter estimations were carried out using non-linear fitting of plasma concentrations-time profiles of the combined PK dataset (i.e., fluorescence-based plasma levels and qRT-PCR based plasma levels) to 2 equations (JMP 10 Software, SAS, Cary, NC; 2 parameter exponential, three parameter exponential). An appropriate pharmacokinetic model was chosen on the basis of lowest sum of weighted squared residuals, lowest Akaike's Information Criterion value, lowest SE of the fitted parameters, and dispersion of the residuals. See Supporting Information for a more detailed description of these methodologies.

#### *Study approval*

The animal research in mice was conducted according to IACUC Protocols 280-12 and 293-10 that were approved by the IACUC of CHLA. All animal care procedures conformed to the Guide for the Care and Use of Laboratory Animals (National Research Council, National Academy Press, Washington DC 1996, USA). Leukaemia cells isolated from de-identified patient specimens were used in the described experiments. The secondary use of leukaemia cells for subsequent laboratory studies did not meet the definition of human subject research per 45 CFR 46.102 (d and f) because it did not include identifiable private information, and the corresponding research protocol CCI-10-00141 was approved

by the CHLA IRB (CCI) (Human Subject Assurance Number: FWA0001914).

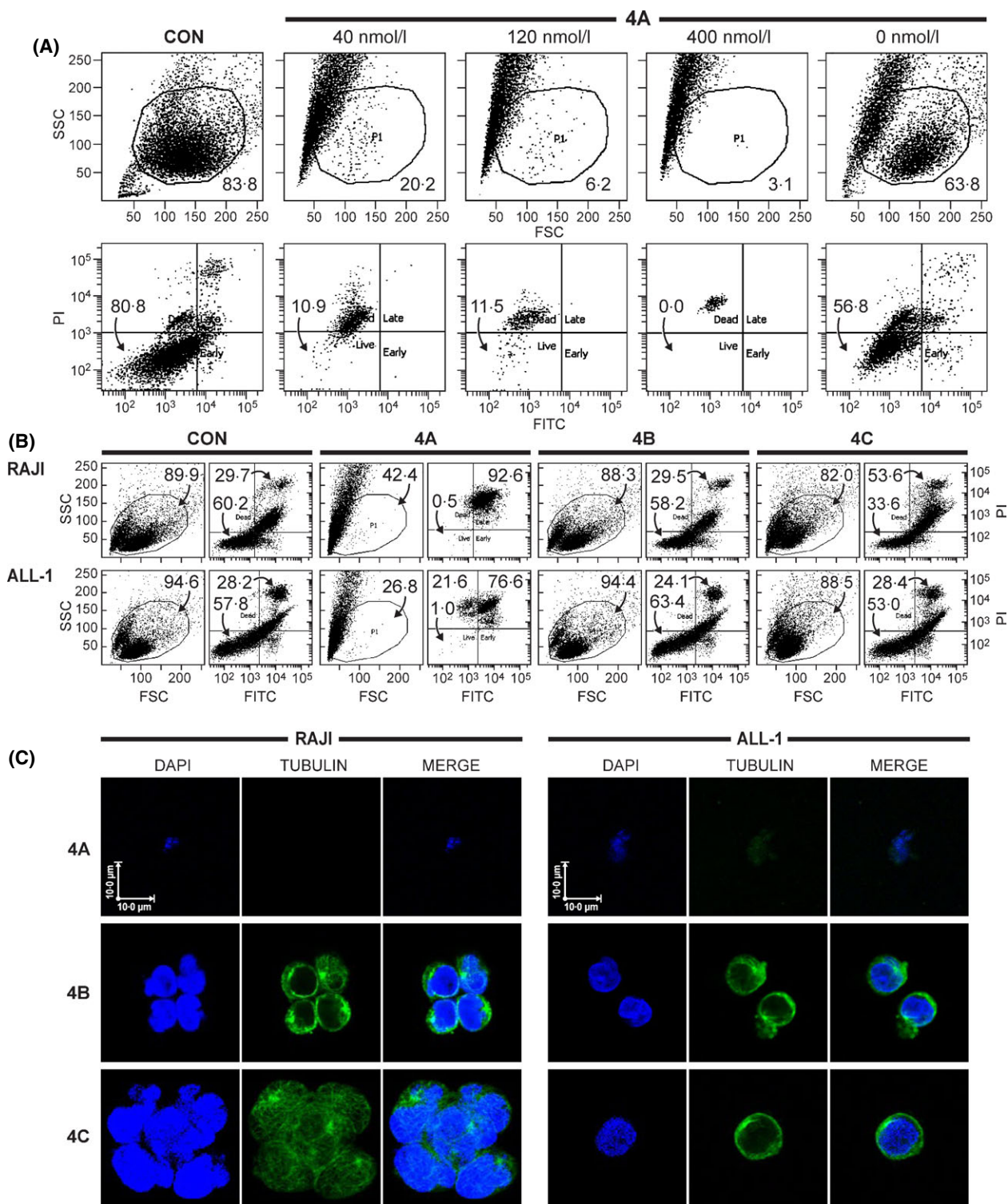
## Results

### *CD22ΔE12 as a molecular target for RNA interference (RNAi) therapy in human B-precursor leukaemia*

We first sought to determine how RNAi with CD22ΔE12-specific siRNA would affect the *in vitro* clonogenicity and proliferation of aggressive patient-derived human BPL xenograft clones isolated from spleens of NOD/SCID mice that had developed overt leukaemia with massive splenomegaly following inoculation with primary leukaemia cells from the respective BPL patients (Uckun *et al*, 2013). Immunophenotyping by multiparameter flow cytometry confirmed the co-expression of multiple BPL-associated human lymphoid differentiation antigens, including high levels of CD10, CD19, and CD34 (Fig 1A) that are recognized markers of putative leukaemic stem cells in BPL. Transfection with CD22ΔE12-siRNA, but not scrambled (scr)-siRNA, caused selective (albeit partial) depletion of CD22ΔE12-mRNA as well as CD22ΔE12-protein in aggressive BPL xenograft cells (Fig 1 B, C). This CD22ΔE12-knockdown was associated with a marked inhibition of their clonogenicity *in vitro* (Fig 1 D, E).

### *CD22ΔE12-siRNA LNF causes selective CD22ΔE12 mRNA depletion and results in loss of the *in vitro* as well as *in vivo* clonogenicity of human B-precursor leukaemia cells*

In order to achieve RNAi in all leukaemic cells in a targeted BPL cell population, we prepared a nanoscale liposomal formulation of CD22ΔE12-siRNA duplex with an encapsulation efficiency of  $96.3 \pm 0.7\%$  and a favourable stability profile both during extended storage at 4°C as well as incubation with mouse or human serum (Figure S1, Figure S2). We examined the ability of the LNF to effectively deliver CD22ΔE12-siRNA into CD22ΔE12<sup>+</sup> human leukaemia cells by using confocal microscopy. The LNF was capable of delivering the Cy3-labelled CD22ΔE12-siRNA into CD22ΔE12<sup>+</sup> human ALL cell lines RAJI (Burkitt leukaemia/B-cell ALL) and ALL-1 (BCR-ABL1<sup>+</sup> BPL), as documented by detection of the internalized CD22ΔE12-siRNA as red-fluorescent foci in the perinuclear cytoplasm as well as the nucleus in all of the cells examined within 4 h of exposure (Fig 2A). The documented nuclear delivery of CD22ΔE12-siRNA confirmed the prerequisite endosomal escape of the siRNA molecules from the internalized liposomes and showed that the CD22ΔE12-siRNA LNF should enable both cytoplasmic post-transcriptional knockdown as well as nuclear transcriptional/co-transcriptional knockdown of the CD22ΔE12 gene expression. In agreement with these observations, treatment of RAJI as well as ALL-1 cells with



*CD22ΔE12*-siRNA LNF (49.5 nmol/l siRNA, 117 μmol/l lipid) resulted in a selective depletion of the target *CD22ΔE12*-mRNA by 48 h (Fig 2B). Neither the scrambled-siRNA containing LNF (90.6 nmol/l siRNA, 117 μmol/l lipid) nor the siRNA-free LNF (0 nmol/l siRNA, 117 μmol/l

lipid) that were included as control LNF affected the *CD22ΔE12*-mRNA levels in RAJI or ALL-1 cells. *CD22ΔE12*-depletion by the *CD22ΔE12*-siRNA formulation was associated with a loss of *in vitro* clonogenicity in both cell lines, while the control formulations did not affect the *in vitro*

**Fig 3.** CD22ΔE12-siRNA LNF causes apoptotic destruction of CD22ΔE12<sup>+</sup> human leukaemia cells. (A & B) Cells were treated for 96 h at 37°C with CD22ΔE12-siRNA LNF (4A, 40 nmol/l–400 nmol/l in [A], 40 nmol/l in [B]), siRNA-free control LNF (4B, 0 nmol/l siRNA), or scr-siRNA LNF (4C, 40 nmol/l). Controls included sham-treated cells (CON) cultured for 96 h. Panel A depicts the results for the ALL-1 cell line, whereas Panel B shows data for both ALL-1 and RAJI. Cells were analysed for apoptosis using the standard quantitative flow cytometric apoptosis assay with the Annexin V-FITC Apoptosis Detection Kit (Sigma, St. Louis, MO, USA; Catalog # APOAF-50TST). The labelled cells were analysed on a LSR II flow cytometer. The anti-leukaemic potency of CD22ΔE12-siRNA LNF is evidenced by the significantly lower percentages of Annexin V-FITC<sup>+</sup>PI<sup>-</sup> live cells located in the left lower quadrant of the corresponding two-colour fluorescence dot plots within the P1 lymphoid window as well as a marked shrinkage and altered SSC as well as decreasing numbers of remaining cells in the P1 lymphoid window in the corresponding forward scatter (FSC)/sideways scatter (SSC) light scatter plot from the 10 000 cells analysed. (C) Confocal images of RAJI and ALL-1 cells analysed in (B) showing nuclear (Blue) destruction and loss of tubulin (Green) cytoskeleton after treatment with the CD22ΔE12-siRNA LNF, 4A.

clonogenic growth of either cell line (Fig 2C). Treatment with CD22ΔE12-siRNA LNF (49.5 nmol/l siRNA, 117 μmol/l lipid) did not affect the clonogenic growth of the CD22ΔE12-negative human DAUDI Burkitt leukaemia/lymphoma cell line (Fig 2D). Thus, the cytotoxic effects of CD22ΔE12-siRNA LNF are dependent on the presence of its molecular target in the treated cell population.

We also used flow cytometric quantitative apoptosis assays to further evaluate the potency of the CD22ΔE12-siRNA LNF against RAJI and ALL-1 cells. As shown in Fig 3A, B, 96-h treatment with CD22ΔE12-siRNA LNF (but not the scr-siRNA LNF) caused apoptosis in both cell lines at a 40 nmol/l concentration. Apoptosis of target leukaemia cells was documented by the significantly lower percentages of Annexin V-FITC<sup>+</sup>PI<sup>-</sup> live cells located in the left lower quadrant of the corresponding two-colour fluorescence dot plots within the P1 lymphoid window. Furthermore, there was a marked shrinkage and altered sideways scatter (SSC) as well as decreasing numbers of remaining cells in the P1 lymphoid window in the corresponding forward scatter (FSC)/SSC light scatter plot from the 10 000 cells analysed. The magnitude of apoptosis was concentration-dependent with no residual viable leukaemia cells remaining at 400 nmol/l (Fig 3A). Confocal images of treated cells confirmed the apoptotic destruction, as documented by an extensive loss of cell integrity, loss of tubulin, cellular shrinkage and nuclear fragmentation (Fig 3C).

We next used blast colony assays in three independent experiments to compare the anti-leukaemic activity of CD22ΔE12-siRNA LNF (49.5 nmol/l × 24 h incubation at 37°C) alone and in combination with standard chemotherapy drugs versus chemotherapy drugs alone against ALL xenograft clones derived from paediatric BPL patients. At this nmol/l concentration, CD22ΔE12-siRNA LNF was significantly more potent than the chemotherapy drugs dexamethasone (DEX) at 25 μmol/l ( $P = 0.033$ ) and pegylated asparaginase (PEG-ASP) at 10 iu/ml ( $P = 0.037$ ) and it was at least as effective as micromolar concentrations of adriamycin (ADR) and vincristine (VCR) (Fig 4). Notably, the combinations of CD22ΔE12-siRNA LNF with DEX, PEG-ASP, ADR and VCR were significantly more effective than the chemotherapy drugs alone. These results demonstrate that chemotherapy-resistant leukaemic clones are not cross-resistant to CD22ΔE12-siRNA LNF and siRNA-mediated CD22ΔE12-

depletion significantly impairs the ability of leukaemic clones to resist the standard chemotherapy drugs.

We next sought to determine how treatment with the CD22ΔE12-siRNA LNF would affect the leukaemia-initiating *in vivo* clonogenic leukaemic cell fraction (viz.: candidate leukaemic stem cell population) in xenograft specimens derived from patients with relapsed BPL. After a 24-h treatment with the CD22ΔE12-siRNA LNF (660 nmol/l), cells were injected intravenously into healthy NOD/SCID mice. Notably, 14 of 15 mice challenged with BPL xenograft cells that were untreated or treated with unformulated CD22ΔE12-siRNA or control liposome formulations 4B and 4C developed overt leukaemia between 78 days and 103 days. Necropsy revealed massive splenomegaly at the time of death (Spleen size:  $2.9 \pm 0.1$  cm) (Fig 5A–C) and histopathological examinations showed evidence of disseminated leukaemia with leukaemic infiltrates in multiple organs, including bone marrow, brain, liver and kidney (Fig 5D, E). By comparison, the spleen size of NOD/SCID mice challenged with CD22ΔE12-siRNA LNF-treated xenograft cells was significantly smaller ( $1.8 \pm 0.3$  cm,  $P = 0.0014$ ) (Fig 5A–C) and histopathological examinations revealed leukaemic cell engraftment in only one of four mice examined ( $P = 0.016$ ) (Fig 5D, E versus F). Thus a single *in vitro* exposure to CD22ΔE12-siRNA LNF to deliver CD22ΔE12-siRNA into leukaemic B-cell precursors in the BPL xenograft specimens was capable of effectively abrogating the *in vivo* clonogenicity of their leukaemia-initiating subpopulations.

#### *In vivo pharmacokinetics and anti-leukaemic potency of the CD22ΔE12-siRNA LNF*

We studied the pharmacokinetics (PK) of CD22ΔE12-siRNA LNF in NOD/SCID mice with xenografted human leukaemia in attempts to determine if effective antileukaemic concentrations can be achieved at nontoxic dose levels. A PK formulation was prepared using Cy3-labelled CD22ΔE12-siRNA and the plasma siRNA levels were determined using fluorescence measurements. Validation experiments were performed using LNF of unlabelled CD22ΔE12-siRNA and a CD22ΔE12-siRNA specific qRT-PCR, as described in Materials and Methods. The composite plasma concentration–time curve of CD22ΔE12-siRNA after the IV injection of a nontoxic, 500 pmol (25 nmol/kg) bolus dose as well as the calculated

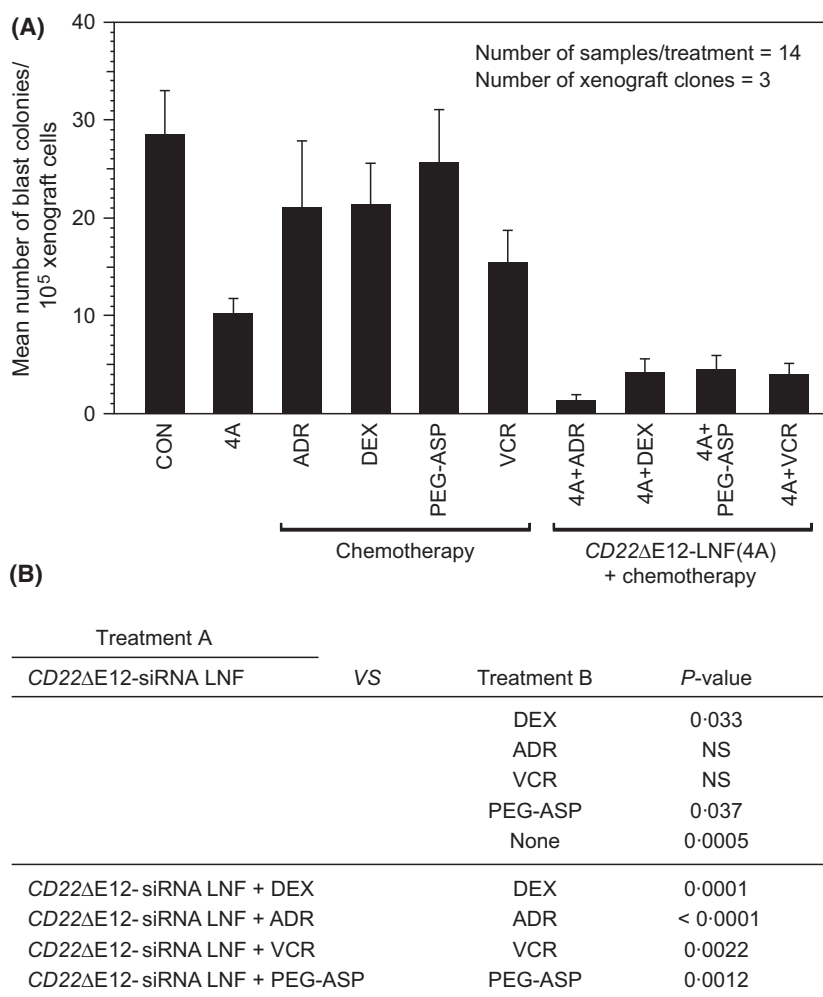


**Fig 4.** *CD22ΔE12*-siRNA augments the potency of standard chemotherapy drugs against patient-derived B-precursor ALL xenograft cells. We examined the potency of *CD22ΔE12*-siRNA LNF (49.5 nmol/l) alone and in combination with standard chemotherapy drugs vs. chemotherapy drugs alone against ALL xenograft clones derived from paediatric BPL patients. (A) Depicted are the cumulative data from three independent experiments. Each bar represents the mean ± SE values from 14 samples (4 replicate samples from Xenograft clone 1, 6 replicate samples from Xenograft clone 2, and 4 replicate samples from Xenograft clone 3). Cells were treated with the respective reagents for 24 h at 37°C. Immediately after treatment, cells (1 × 10<sup>5</sup> cells/ml) were suspended in alpha-MEM supplemented with 0.9% methylcellulose, 30% foetal calf serum and 2 mmol/l L-glutamine. We used the standard chemotherapy drugs commonly used in BPL therapy, including vincristine (VCR, 11 μmol/l), adriamycin/doxorubicin (ADR, 17 μmol/l), pegylated-asparaginase (PEG-ASP, oncospar; 10 iu/ml), dexamethasone (DEX, 25 μmol/l). The chemotherapy drugs were obtained from the Pharmacy of the Children’s Hospital Los Angeles. The following concentrations were used in treatments: 49.5 nmol/l *CD22ΔE12*-siRNA LNF (117 μmol/l lipid), 90.6 μmol/l scr-siRNA LNF (117 μmol/l lipid), 11 μmol/l VCR, 10 IU PEG-ASP, 17 μmol/l DOX, 25 μmol/l DEX. Controls included untreated cells and, in some experiments, cells treated with siRNA-free LNF (0 nmol/l siRNA, 117 μmol/l lipid). 4 or 6 replicate 1 ml samples containing 0.5 × 10<sup>6</sup> cells/sample were cultured in 35 mm Petri dishes for 7 days at 37°C in a humidified 5% CO<sub>2</sub> atmosphere. On day 7, colonies containing ≥20 cells were counted using an inverted Nikon Eclipse TS100 microscope. (B) depicts the statistical comparisons between various treatment groups using non-parametric Wilcoxon/Mann–Whitney tests on ranked values for each pair of treatments. *CD22ΔE12*-siRNA LNF alone significantly reduced the colony counts compared to DEX (*P* = 0.033) and PEG-ASP (*P* = 0.037). Significant reductions in colony counts were observed compared to control for *CD22ΔE12*-siRNA LNF (*P* = 0.0005), ADR (*P* = 0.039) and VCR (0.016), but not for DEX (*P* = 0.15) or PEG-ASP (0.56). *CD22ΔE12*-siRNA LNF in combination with ADR (*P* < 0.0001), DEX (*P* = 0.0001), PEG-ASP (*P* = 0.0012) or VCR (*P* = 0.0022) was more effective in abrogating colony counts than treatment of ADR, DEX, PEG-ASP or VCR alone. *CD22ΔE12*-siRNA LNF in combination with ADR (*P* < 0.0001), DEX (*P* = 0.0075), PEG-ASP (*P* = 0.011) or VCR (*P* = 0.0044) was more effective in abrogating colony counts than treatment of *CD22ΔE12*-siRNA LNF alone.

PK parameter values are shown in Fig 6A. A 3-parameter exponential decay pharmacokinetic model was fit to the plasma concentration–time curves, and the calculated pharmacokinetic parameter values are shown in Fig 6A. Peak plasma concentrations of *CD22ΔE12*-siRNA LNF in excess of

50 nmol/l, which is highly effective against human BPL cells, could be easily achieved at this dose level. The predicted maximum plasma concentration (*C*<sub>max</sub>) was 81 ± 14 nmol/l and the systemic exposure (area under the curve [AUC])<sub>0–24 h</sub> at this dose level was 297 nmol/l.h

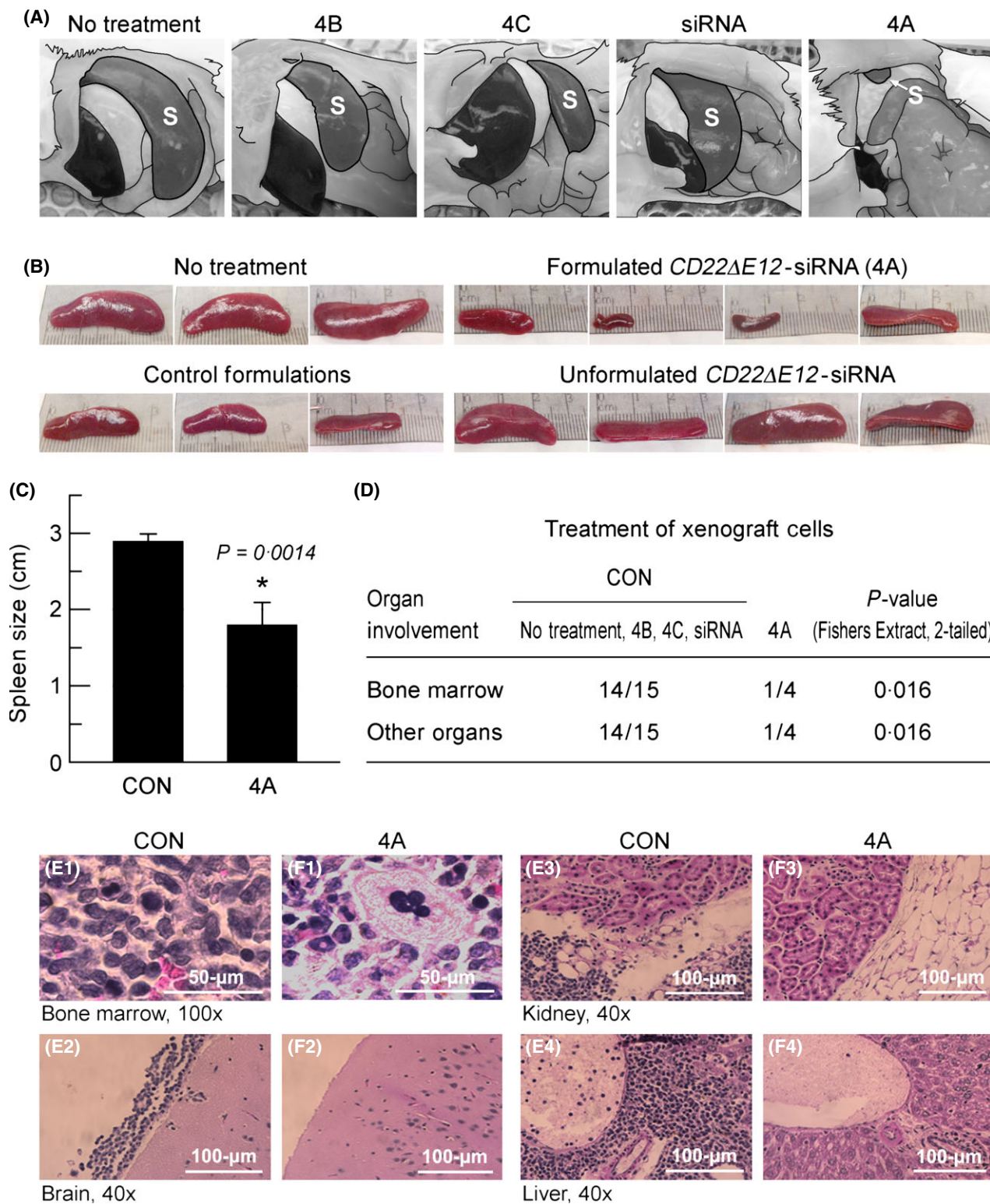
(AUMC 0–24 h = 2364 nmol/l. h<sup>2</sup>) (Fig 6A–D). The estimated mean residence time (MRT) (AUMC/AUC) was 8 h and the plasma half-life (= MRT × 0.693) was 5.5 h.

We next evaluated the *in vivo* anti-leukaemic activity of the CD22ΔE12-siRNA LNF in NOD/SCID mouse xenograft models of relapsed BPL. All untreated control NOD/SCID mice challenged with an intravenous inoculum of xenograft cells derived from two different relapsed BPL patients developed rapidly progressive disseminated leukaemia and either died or were electively killed in moribund condition due to their advanced leukaemia within 125 days with a median EFS time of only 116 days. Treatment with the LNF of scr-siRNA (25 nmol/kg/day × 3 days, days 1–3) or an empty LNF not containing any siRNA did not alter this aggressive course of disease and all mice on this control treatment regimen died of overt leukaemia with a median EFS of 107 days (Fig 6E). In contrast, the median EFS time was more than doubled for the 19 test mice that were treated with the LNF of CD22ΔE12-siRNA at two different dose levels (EFS >250 d on the low-dose regimen = 2.5 nmol/kg per day × 3 days, days 1–3, *n* = 10); EFS >250 days on the high-dose regimen = 25 nmol/kg per day × 3 days, days 1–3, *n* = 9) (*P*-value: <0.0001) (Fig 6E, F). Mice treated at the higher dose level of CD22ΔE12-siRNA LNF had a better EFS outcome than mice treated at the lower dose level: Their proportion remaining alive free of leukaemia-associated morbidity at 200 days (*viz.*: 89%) was above the higher confidence interval (CI) value for the lower dose group (95%CI = 22–82%). Whereas none of the control mice was alive after 125 days, 76 ± 15% of NOD/SCID mice that were treated with the LNF of CD22ΔE12-siRNA at the higher dose level (25 nmol/kg per day × 3 days) remained alive with no evidence of leukaemia-associated morbidity at 250 days after inoculation with an invariably fatal dose of highly aggressive human BPL xenograft cells (Fig 6E, F). These results illustrate that the mutant CD22ΔE12 mRNA would be an excellent molecular target for RNAi therapy against BPL.

Forced expression of CD22ΔE12 in transgenic (Tg)-mice causes fatal CD19<sup>+</sup>CD24<sup>+</sup>CD45R/B220<sup>+</sup>CD127/IL7-R<sup>+</sup>sIgM<sup>-</sup> BPL at a median age of 190 days, indicating that CD22ΔE12 alone is sufficient for malignant transformation and clonal expansion of B-cell precursors in mice (Figure S3–S8). By using a combination of FISH and SKY, the approximate chromosomal band locations of the human CD22ΔE12 transgene in BPL cells from CD22ΔE12-Tg mice were identified on 18D (detected only in 11 of 31 metaphases) and 19C2 (Figure S5, Figure S8). SKY revealed a predominant clone with a normal diploid karyotype and two subclones with abnormal karyotypes: 40,XX [21]/41,XX, +3[3]/40,XX, Der (13)T(10D2,13D2)[7] (Figure S5 A–D). PCR-based clonality assays confirmed the clonal origin of the CD22ΔE12-Tg BPL cells and showed that the *IGH* locus of their immunoglobulin genes was aberrantly rearranged with a noncanonical incomplete V<sub>H</sub>(D)<sub>H</sub> recombination (Figure S5 E–G) (Accession # LM652707). The presence of the CD22ΔE12 transgene

was further confirmed by genomic PCR using a panel of 10 separate primer pairs recognizing different segments of the transgene (Figure S8 B–E). By using RT-PCR with a 5' CD22ΔE12 E10 primer (E10–F) and a 3' vector backbone primer (CD22ΔE12Tg-R2) to amplify a segment of the transgene message spanning CD22ΔE12 exons 10, 11, 13 and 14, the expression of the CD22ΔE12 transcript was confirmed in BPL cells from leukaemic CD22ΔE12-Tg mice as well as splenocytes from pre-leukaemic CD22ΔE12-Tg mice (Figure S8 F1). The expression of the CD22ΔE12 protein in CD22ΔE12-Tg BPL cells was confirmed by Western blot analysis (Figure S8 F2) as well as confocal fluorescence microscopy examination of frozen sections of bone marrow from leukaemic mice (Figure S8 G).

Inoculation of NOD/SCID mice with 2 × 10<sup>6</sup> leukaemia cells from CD22ΔE12-Tg mice invariably caused fatal BPL with a median leukaemia-free survival time of only 26 days (Figure S9). Leukaemic NOD/SCID recipients developed massive splenomegaly with very high spleen cell counts (Figure S9B), replacement of normal splenocytes by CD19<sup>+</sup>CD45R/B220<sup>+</sup>CD127/IL7-R<sup>+</sup> BPL (Figure S9C) and leukaemic infiltration of bone marrow, kidney/perirenal adipose tissue, CNS and liver (Figure S9 D1–D4), reminiscent of the fatal BPL in NOD/SCID mice caused by inoculation of CD22ΔE12<sup>+</sup> human BPL cells. A 24-h pretreatment with CD22ΔE12-siRNA LNF (200 nmol/l) markedly impaired the ability of the CD22ΔE12-Tg mouse BPL cells to initiate leukaemia in NOD/SCID mice, reminiscent of its effects on leukaemia-initiating human BPL xenograft cells in NOD/SCID mice. No detailed *in vitro* experiments were performed with the CD22ΔE12-Tg BPL cells as they don't grow *in vitro* and >99% die spontaneously at 36–48 h. Notably, 10 of 10 mice challenged with 1 × 10<sup>6</sup> CD22ΔE12-Tg BPL cells that were untreated or treated with the scr-siRNA containing control liposome formulation developed overt leukaemia on day 12 after leukaemic cell inoculation. Necropsy revealed massive splenomegaly at the time of death (Spleen size/cell count [× 10<sup>6</sup>]: 2.5 ± 0.3 cm/626 ± 53 for mice receiving untreated BPL cells and 2.3 ± 0.2 cm/227 ± 20 for mice receiving BPL cells treated with scr-siRNA LNF). In contrast, none of the five mice receiving CD22ΔE12-Tg BPL cells that were treated with CD22ΔE12-siRNA LNF had evidence of overt leukaemia on day 12. Their spleen sizes were normal (Figure S10 A) and their spleen cell counts were significantly lower than those of control mice challenged with untreated or scr-siRNA LNF-treated BPL cells (Figure S10 B). These findings provide direct experimental evidence that CD22ΔE12-directed RNAi *in vivo* initiated by a 24-h *in vitro* exposure to the CD22ΔE12-siRNA formulation 4A severely damages the *in vivo* clonogenic fraction of the mouse BPL cells derived from CD22ΔE12-Tg mice BPL and abrogates their ability to engraft and initiate leukaemia in NOD/SCID mice. We next set out to determine if CD22ΔE12-siRNA LNF could improve the EFS outcome of NOD/SCID mice challenged with a very aggressive BPL clone derived from



leukaemia cells of a CD22ΔE12-Tg mouse with BPL. Notably, CD22ΔE12-siRNA LNF (2.5 nmol/kg per day × 3 days) significantly improved the EFS outcome of NOD/SCID mice challenged with these aggressive mouse BPL cells derived from CD22ΔE12-Tg mice ( $P < 0.0001$  versus untreated mice

or mice treated with scr-siRNA LNF) (Figure S10 C&D). Calculation of the 95% CIs at three time points (viz.: 25, 30 and 35 days after inoculation of leukaemia cells) showed increased survival for the CD22ΔE12-siRNA LNF treatment compared to the upper 95% CI for the combined group of

**Fig 5.** CD22ΔE12-siRNA loaded nanoscale liposomal formulation 4A (660 nmol/l × 24h) abrogates the ability of *in vivo* clonogenic BPL xenograft cells to engraft and initiate leukaemia in NOD/SCID mice. (A & B) We observed massive splenomegaly in NOD/SCID mice that invariably developed disseminated leukaemia after iv injection of B-precursor ALL xenograft cells that were either untreated or treated for 24 h at 37°C with unformulated CD22ΔE12-siRNA (660 nmol/l) or control formulations 4B (same lipid as in 4A but no siRNA) and 4C (1.2 μmol/l scr-siRNA). Test mice were inoculated with xenograft cells that were treated with the CD22ΔE12-siRNA LNF 4A (660 nmol/l for 24 h). In the preparation of the two mouse diagrams in A, the artist used colour photographs taken at the time of necropsy. Scans of the photos were used to accurately trace the contours of organ structures and mouse outlines. S, spleen. The spleen images in B were obtained using an iPhone 4S equipped with an 8-megapixel iSight camera. (C & D) The cumulative data on spleen size are shown in C. Statistical comparisons of diffuse organ infiltration data are shown in D. One mouse inoculated with untreated xenograft cells developed CNS leukaemia without evidence of other organ involvement except for few clusters of leukaemic blasts in the bone marrow. One of the control mice (CON) receiving 4C-treated xenograft cells showed only bone marrow involvement. Notably, 14 of 15 mice challenged with BPL xenograft cells that were untreated or treated with unformulated CD22ΔE12-siRNA or control liposome formulations 4B and 4C developed overt leukaemia between 78 and 103 days. Necropsy revealed massive splenomegaly at the time of death (Spleen size: 2.9 ± 0.1 cm) and histopathological examinations showed evidence of disseminated leukaemia with leukaemic infiltrates in multiple organs, including bone marrow, brain, liver and kidney. By comparison, the spleen size of NOD/SCID mice challenged with 4A-treated xenograft cells was significantly smaller (1.8 ± 0.3 cm,  $P = 0.0014$ ) and histopathological examinations revealed leukaemic cell engraftment in only one of four mice examined ( $P = 0.016$ ). These findings provide direct experimental evidence that CD22ΔE12-directed RNAi *in vivo* initiated by a 24-h *in vitro* exposure to the CD22ΔE12-siRNA formulation 4A severely damages the *in vivo* clonogenic fraction in xenograft cell populations derived from patients with aggressive BPL and abrogates their ability to engraft and initiate leukaemia in NOD/SCID mice. (E & F) Depicted are representative results obtained using xenograft cells derived from a relapsed paediatric BPL patient. The histopathology images of H&E stained tissue slides in E1-E4 (control, [CON]) versus F1-F4 (4A) illustrate the presence of leukaemic infiltrates in the organs of a mouse from the CON group that received untreated xenograft cells versus their absence in the organs of a mouse from the CD22ΔE12-siRNA LNF/4A pretreatment group. \*Difference from CON statistically significant.

scr-siRNA LNF treated and untreated control mice (Survival at 25, 30 and 35 days for CD22ΔE12-siRNA LNF treated mice was 90% (upper 95% CI for the combined control = 48%), 90% (upper 95% CI for the combined control = 43%) and 40% (upper 95% CI for the combined control = 28%), respectively.

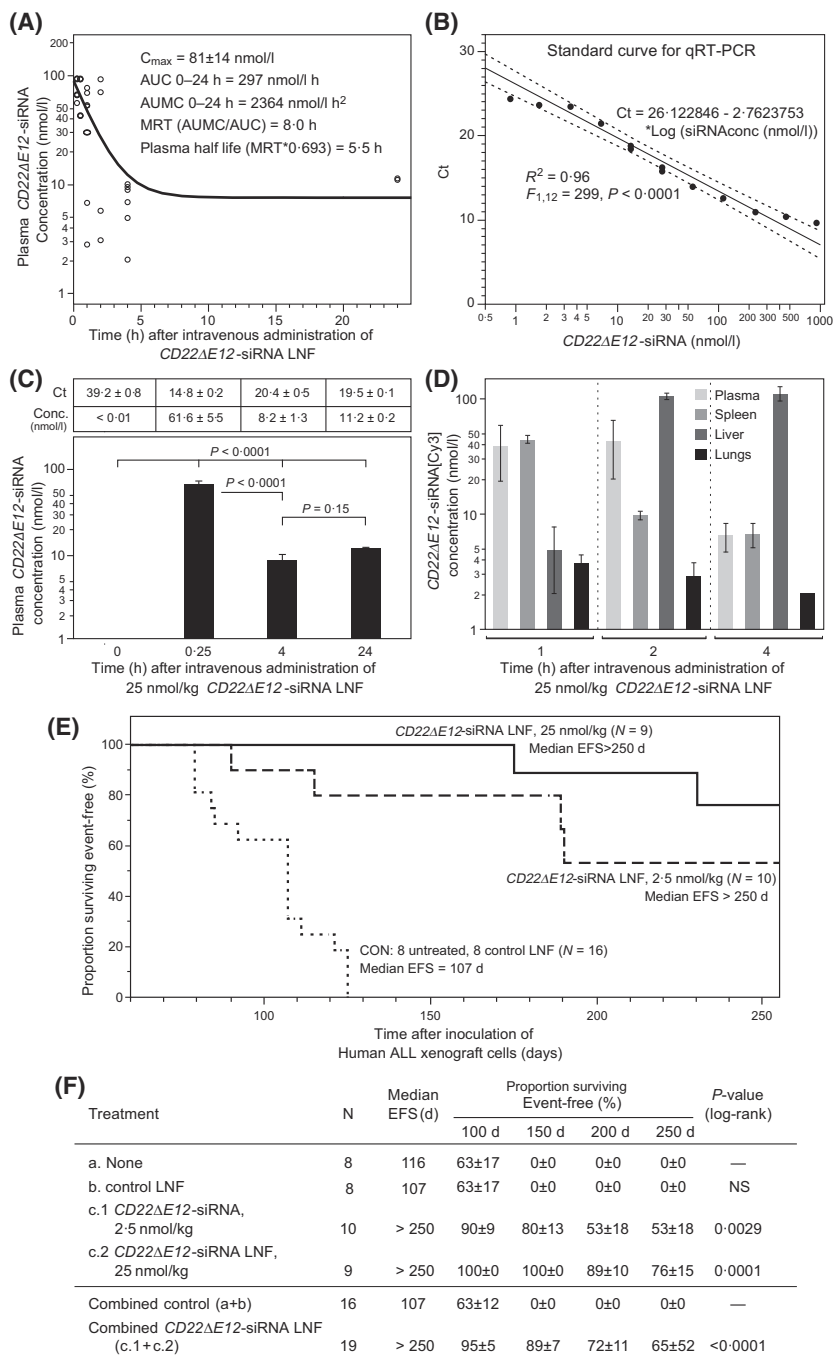
## Discussion

The major challenge in the treatment of BPL is to cure patients who have relapsed despite intensive frontline chemotherapy (Reaman, 2004; Gaynon, 2005; Seibel, 2011; Hastings *et al*, 2014). There is an urgent and unmet need to identify new drug candidates capable of destroying chemotherapy-resistant leukaemic B-cell precursors (BCP). The CD22ΔE12 genetic defect in CD22 expression is found in the vast majority of relapsed BPL cases, newly diagnosed infant BPL cases and newly diagnosed high-risk paediatric BPL cases (Uckun *et al*, 2014). Our studies using quantitative real time RT-PCR on samples obtained from newly diagnosed high-risk paediatric BPL patients demonstrated that 89% of paediatric cases and 100% of infant cases were CD22ΔE12<sup>+</sup>. Using multiprobe CD22 gene expression profiling, we confirmed the high incidence of CD22ΔE12 in genetically defined high-risk BPL subsets, i.e., 97% of *TCF3 (E2A)-PBX1*<sup>+</sup> ( $n = 61$ ,  $P < 0.0001$ ), 82% of *KMT2A (MLL)*-rearranged (R)<sup>+</sup> ( $n = 95$ ,  $P < 0.0001$ ) and 85% of *BCR-ABL1*<sup>+</sup> BPL cases ( $n = 123$ ,  $P < 0.0001$ ) (Uckun *et al*, 2014). Our overarching objective in this project was to design an innovative and effective strategy that would utilize the CD22ΔE12 genetic lesion as a molecular target to gain a therapeutic advantage against chemotherapy-resistant aggressive BPL. Specifically, we sought to validate CD22ΔE12 as an effective molecular target for RNA interference (RNAi) therapy in BPL. The potent *in vitro* and

*in vivo* anti-leukaemic activity of the LNF of CD22ΔE12-siRNA against human leukaemia cells from relapsed BPL patients provided the first preclinical proof-of-concept for a potentially paradigm-shifting innovative strategy for the treatment of relapsed BPL patients, whereby the chemotherapy resistant leukaemic clones could be destroyed using nanoformulations of CD22ΔE12-specific siRNA as a new class of RNAi therapeutics. The ability of CD22ΔE12-siRNA LNF to augment the anti-leukaemic potency of standard chemotherapy drugs further underlines the translational potential of this strategy.

Nanoparticles represent particularly attractive delivery systems for anti-sense oligonucleotides and siRNA and may provide the foundation for rational design and formulation of RNAi-triggering nanomedicines (Gokhale *et al*, 2002; Farrell *et al*, 2011; Guo & Huang, 2011; Haque *et al*, 2012; Karve *et al*, 2012; Uckun *et al*, 2013; Shu *et al*, 2014). A LNF of CD22ΔE12-specific siRNA was developed as an RNAi therapeutic candidate against BPL and its ability to cause CD22ΔE12 depletion in primary BPL cells and abrogate their clonogenicity both *in vitro* and *in vivo* was confirmed. We used a mixture of the cationic lipid 2,3-dioleoyloxypropyltrimethylammonium chloride (DOTAP) and the neutral lipid 1,2-dioleoyl-sn-glycero-3-phosphoethanolamine (DOPE) in the preparation of the LNF. Both of these lipid components have been previously used in clinical nanoformulations with favourable patient safety profiles (Chang *et al*, 2012; Uckun & Yiv, 2012). Further development and optimization of this RNAi therapeutic candidate targeting CD22ΔE12 may facilitate a paradigm shift in therapy of relapsed BPL.

The expression of CD22 on leukaemic B-cell precursors has motivated the development and clinical testing of CD22-directed monoclonal antibody (MoAb), recombinant fusion toxins and antibody-drug conjugates as therapeutic agents against



BPL in children (D’Cruz & Uckun, 2013). However, these therapeutic modalities all target the surface epitopes of CD22 and do not discriminate between normal B-cells expressing intact CD22 and BPL cells expressing CD22ΔE12. Due to the presence of CD22 on normal human B-cells and B-cell precursors, lymphotoxicity with reduced B-cell numbers and possible hypogammaglobulinemia with an increased risk of infections would be anticipated side effects of CD22-directed MoAb and MoAb-based therapeutics in clinical settings. In contrast, RNAi therapeutics targeting CD22ΔE12 would only kill BPL cells

while leaving normal B-cell precursors and B-cells with an intact CD22 encoded by a wildtype CD22 mRNA unharmed. The specificity of CD22ΔE12-siRNA LNF for the CD22ΔE12-mRNA positive leukaemia cells was confirmed in this study by showing that CD22<sup>+</sup> DAUDI Burkitt lymphoma/leukaemia cells are not killed by this nanoformulation because they do not harbour the CD22ΔE12 molecular target. In contrast to the CD22ΔE12- DAUDI cell line, both CD22ΔE12<sup>+</sup> ALL cell lines RAJI and ALL-1, as well as each of the 6 CD22ΔE12<sup>+</sup> BPL xenograft clones, were killed by CD22ΔE12-siRNA LNF.

**Fig 6.** *In Vivo* Pharmacokinetics, Biodistribution and Anti-Leukaemic Potency of CD22ΔE12-siRNA LNF. (A–C) Plasma concentration–time profile of CD22ΔE12-siRNA LNF in NOD/SCID mice with xenografted human BPL after a single iv bolus injection of CD22ΔE12-siRNA LNF (25 nmol/kg). Depicted is the plasma concentration–time curve that was generated using the combined dataset generated using two different pharmacokinetic (PK) formulations, as described in Materials and Methods. The first formulation was prepared using the Cy3-labelled CD22ΔE12-siRNA and the Cy3-based fluorescence of the plasma samples was measured using the Synergy HT Biotek fluorescence microplate reader. A second formulation used unlabelled siRNA for which we used a quantitative(q) RT-PCR technique to measure the CD22ΔE12-specific siRNA levels in plasma samples. A 3-parameter exponential decay pharmacokinetic model was fit to the plasma concentration–time curves, and the calculated PK parameter values are shown (A) In evaluation of the PK samples from mice that received the LNF of unlabelled CD22ΔE12-siRNA (B, C), small RNA species were isolated using the mirVana™ miRNA isolation Kit (Invitrogen/Life Technologies). The qPCR reaction was performed in the Applied Biosystems 7900HT Fast Real-Time PCR System using a TaqMan® Universal PCR Master Mix II, no UNG (Invitrogen/Life Technologies), custom-designed specific FAM probe and primer mixture, and the RT reaction product. We used an RT stem loop primer (<https://www.lifetechnologies.com/order/custom-genomic-products/tools/smallrna/>) that was custom designed specifically to anneal the 3'-end of the sense strand of the target CD22ΔE12-siRNA duplex (Invitrogen/Life Technologies). A standard curve was generated for the qRT-PCR assay using naked CD22ΔE12-siRNA (B). (D) Bar graphs showing the plasma versus organ distribution of the CD22ΔE12-siRNA LNF at 1 h and 2 h versus 4 h after iv administration (25 nmol/kg). The LNF of the Cy3-labelled CD22ΔE12-siRNA was used [E] Depicted are the EFS curves of NOD/SCID mice that were inoculated i.v. with xenograft cells ( $4 \times 10^5$  cells/mouse) derived from primary leukaemia cells of two paediatric patients with BPL. The EFS curves were generated using the Kaplan-Meier product limit method. Sixteen control mice were either left untreated or treated with the liposomal control nanoformulation of scr-siRNA (25 nmol/kg per day  $\times$  3 days, days 1–3) or an empty control LNF. Test mice were treated with the CD22ΔE12-siRNA LNF (Low-dose regimen = 2.5 nmol/kg per day  $\times$  3 days, days 1–3,  $n = 10$ ; High-dose regimen = 25 nmol/kg per day  $\times$  3 days, days 1–3,  $n = 9$ ). Each of the 16 control mice developed fatal leukaemia within 125 days with a massive splenomegaly (spleen size:  $3.4 \pm 0.1$  cm for untreated mice,  $3.2 \pm 0.1$  cm for mice treated with control LNF; nucleated spleen cell count:  $564 \pm 203 \times 10^6$  ( $\text{Log}_{10} = 8.6 \pm 0.2$ ) for untreated control mice and  $828 \pm 98 \times 10^6$  ( $\text{Log}_{10} = 8.9 \pm 0.1$ ) for mice treated with control LNF. Their spleen size and cellularity were markedly greater than those of non-leukaemic control NOD/SCID mice that had not been inoculated with any leukaemia cells (spleen size  $1.3 \pm 0.1$  cm, (*T*-test, Unequal variances,  $\text{Log}_{10}$  transformed data,  $P < 0.0001$ ); Nucleated spleen cell count =  $4.6 \pm 0.4 \times 10^6$  ( $\text{Log}_{10} = 6.7 \pm 0.04$ ),  $P < 0.0001$ ). CD22ΔE12-siRNA LNF significantly improved the EFS outcome at both dose levels tested. (F) Life table statistics for the EFS curves shown in (E).

## Acknowledgments

The project described was supported in part by the Keck School of Medicine Regenerative Medicine Initiative Award (F.M.U) and by DHHS grants P30CA014089 (F.M.U), U01-CA-151837 (F.M.U), R01CA-154471 (F.M.U) from the National Cancer Institute (F.M.U). J. C. acknowledges the support from NIH (Director's New Innovator Award 1DP2OD007246-01). The content is solely the responsibility of the authors and does not necessarily represent the official views of the National Cancer Institute or the National Institutes of Health. This work was also supported in part by Nautica Triathlon and its producer Michael Epstein (F.M.U), Couples Against Leukaemia Foundation (F.M.U) and Saban Research Institute Merit Awards (F.M.U). We thank Mrs. Parvin Izadi of the CHLA Bone Marrow Laboratory, Mrs. Tsen-Yin Lin of the CHLA FACS Core as well as Ernesto Barron and Anthony Rodriguez of the USC Norris Comprehensive Cancer Center Cell and Tissue Imaging Core for their assistance. We thank Dr. Jerry Adams (WEHI, Melbourne, Australia) for the pEμ-SR plasmid and Dr. Zanzian Xia (School of Biological Science and Technology, Central South University, Changsha, Hunan 410078, China) for the lentiviral vector pCL6-2AEGwo. We thank S. Yiv from the Children's Hospital Los Angeles for preparing liposomal formulations of siRNA. We thank Julie Koeman (Van Andel Institute, Michigan) for spectral karyotyping and FISH. We thank the technicians of the Uckun laboratory, including Anoush Shahidzadeh, Ingrid Cely, Erika Olson, Rita Ishkhanian and Martha Arellano for their assistance throughout the study. We also thank Drs. Amanda Termuhlen and Paul

Gaynon from the USC Keck School of Medicine for providing primary BPL specimens.

## Authorship contribution

All authors have made significant and substantive contributions to the study. All authors reviewed and revised the paper. F.M.U. was the NIH-funded Principal Investigator who designed, directed and supervised this study and wrote the final manuscript. S.Q. performed the bioinformatics and statistical analyses. H.M. performed multiple experiments with siRNA and siRNA formulations and collected data. In addition, H.M. performed PCR and RT-PCR on blood samples, splenocytes and BPL cells from CD22ΔE12-Tg mice. J.C. and D.E.M. contributed to the characterization of the LNF.

## Conflict-of-interest disclosure

The authors declare no competing financial interests.

## Supporting Information

Additional Supporting Information may be found in the online version of this article:

**Data S1.** Supplemental methods

**Table S1.** Primers used for PCR screening and sequence verification of the CD22ΔE12-cDNA insertion

**Figure S1.** CD22ΔE12 siRNA Liposomal Nanoformulation (LNF)

**Figure S2.** Serum stability of CD22ΔE12-siRNA LNF [A].

**Figure S3.** Preparation of the pEμ-SR-CD22ΔE12 vector

for microinjection.

**Figure S4.** *CD22* $\Delta$ E12-Transgenic (Tg) Mice Develop Fatal B-precursor Leukemia (BPL).

**Figure S5.** FISH, SKY and PCR Analyses of *CD22* $\Delta$ E12-Tg Leukemia cells.

**Figure S6.** Primer Sets and Assay Conditions for Genomic PCR and RT-PCR.

**Figure S7.** Lentiviral Construct with *CD22* $\Delta$ E12-14 Insert.

**Figure S8.** Characterization of *CD22* $\Delta$ E12-Tg Leukemia Cells.

**Figure S9.** *CD22* $\Delta$ E12-Tg BPL cells cause fatal leukemia in NOD/SCID mice.

**Figure S10.** Anti-leukemic activity of *CD22* $\Delta$ E12-siRNA LNF against murine BPL cells from *CD22* $\Delta$ E12-transgenic mice.

## References

- Chang, H.-I., Cheng, M.-Y. & Yeh, M.-K. (2012) Clinically-proven liposome-based drug delivery: formulation, characterization and therapeutic efficacy. *Open Access Scientific Reports*, **1**, 1–8.
- D’Cruz, O.J. & Uckun, F.M. (2013) Novel mAb-based therapies for leukemia. In: “Monoclonal Antibodies in Oncology” (ed. by F.M. Uckun), Future Medicine 2013, pp. 54–77. Future Medicine Ltd, London. doi: 10.2217/ebo.13.218
- Farrell, D., Ptak, K., Panaro, N.J. & Grodzinski, P. (2011) Nanotechnology-based cancer therapeutics—promise and challenge—lessons learned through the NCI Alliance for Nanotechnology in Cancer. *Pharmaceutical Research*, **28**, 273–278.
- Gaynon, P.S. (2005) Childhood ALL and relapse. *British Journal of Haematology*, **131**, 579–587.
- Gokhale, P.C., Zhang, C., Newsome, J.T., Pei, J., Ahmad, I., Rahman, A. & Dritschilo, A. (2002) Pharmacokinetics, toxicity, and efficacy of end-modified raf antisense oligodeoxyribonucleotide encapsulated in a novel cationic liposome. *Clinical Cancer Research*, **8**, 3611–3621.
- Haque, F., Shu, D., Shu, Y., Shlyakhtenko, L.S., Rychahou, P.G., Evers, B.M. & Guo, P. (2012) Ultrastable synergistic tetravalent RNA nanoparticles for targeting to cancers. *Nano Today*, **7**, 245–257.
- Hastings, C., Gaynon, P.S., Nachman, J.B., Sather, H.N., Lu, X., Devidas, M. & Seibel, N.L. (2014) Increased post-induction intensification improves outcome in children and adolescents with a markedly elevated white blood cell count ( $\geq 200 \times 10^9/l$ ) with T cell acute lymphoblastic leukaemia but not B cell disease: a report from the Children’s Oncology Group. *British Journal of Haematology*. doi: 10.1111/bjh.13160 [Epub ahead of print]
- Karve, S., Werner, M.E., Sukumar, R., Cummings, N.D., Copp, J.A., Wang, E.C., Li, C., Sethi, M., Chen, R.C., Pacold, M.E. & Wang, A.Z. (2012) Revival of the abandoned therapeutic wortmannin by nanoparticle drug delivery. *Proceedings of the National Academy of Sciences of the United States of America*, **109**, 8230–8235.
- Ma, H., Qazi, S., Ozer, Z., Gaynon, P. & Uckun, F.M. (2012) *CD22* Exon 12 deletion is a characteristic genetic defect of therapy-refractory clones in paediatric acute lymphoblastic leukaemia. *British Journal of Haematology*, **156**, 89–98.
- Myers, D., Yiv, S., Qazi, S., Ma, H., Cely, I., Shahidzadeh, A., Arellano-Garcia, M., Finestone, E., Gaynon, P., Termuhlen, A., Cheng, J. & Uckun, F.M. (2014) *CD19*-antigen specific nanoscale liposomal formulation of a SYK P-site inhibitor causes apoptotic destruction of human B-precursor leukemia cells. *Integr Biol (Camb)*. **2014** Aug;6(8): 766–80. doi: 10.1039/c4ib00095a.
- Reaman, G.H. (2004) Pediatric cancer research from past successes through collaboration to future transdisciplinary research. *Journal of Pediatric Oncology Nursing*, **21**, 123–127.
- Seibel, N.L. (2011) Survival after relapse in childhood acute lymphoblastic leukemia. *Clinical Advances in Hematology & Oncology*, **9**, 476–478.
- Shu, Y., Pi, F., Sharma, A., Rajabi, M., Haque, F., Shu, D., Leggas, M., Evers, B.M. & Guo, P. (2014) Stable RNA nanoparticles as potential new generation drugs for cancer therapy. *Advanced Drug Delivery Reviews*, **66**, 74–89.
- Uckun, F.M. & Yiv, S. (2012) Nanoscale small interfering RNA delivery systems for personalized cancer therapy. *International Journal of Nano Studies & Technology*, **1**, 2.
- Uckun, F.M., Goodman, P., Ma, H., Dibirdik, I. & Qazi, S. (2010a) *CD22* Exon 12 deletion as a novel pathogenic mechanism of human B-precursor leukemia. *Proceedings of the National Academy of Sciences of the United States of America*, **107**, 16852–16857.
- Uckun, F.M., Qazi, S., Ma, H., Tuel-Ahlgren, L. & Ozer, Z. (2010b) STAT3 is a substrate of SYK tyrosine kinase in B-lineage leukemia/lymphoma cells exposed to oxidative stress. *Proceedings of the National Academy of Sciences of the United States of America*, **107**, 2902–2907.
- Uckun, F.M., Qazi, S., Ozer, Z., Garner, A.L., Pitt, J., Ma, H. & Janda, K.D. (2011) Inducing apoptosis in chemotherapy-resistant B-lineage acute lymphoblastic leukaemia cells by targeting HSPA5, a master regulator of the anti-apoptotic unfolded protein response signalling network. *British Journal of Haematology*, **153**, 741–752.
- Uckun, F.M., Ma, H., Zhang, J., Ozer, Z., Dovat, S., Mao, C., Ishkhanian, R., Goodman, P. & Qazi, S. (2012) Serine phosphorylation by SYK is critical for nuclear localization and transcription factor function of Ikaros. *Proceedings of the National Academy of Sciences of the United States of America*, **109**, 18072–18077.
- Uckun, F.M., Qazi, S., Cely, I., Sahin, K., Shahidzadeh, A., Ozercan, I., Yin, Q., Gaynon, P., Termuhlen, A., Cheng, J. & Yiv, S. (2013) Nanoscale liposomal formulation of a SYK P-site inhibitor against B-precursor leukemia. *Blood*, **121**, 4348–4354.
- Uckun, F.M., Qazi, S., Ma, H. & Mitchell, L. (2014) *CD22* $\Delta$ E12 as a molecular target for corrective repair using a RNA trans-splicing strategy: anti-leukemic activity of a rationally designed RNA trans-splicing molecule. *Integrative Biology (Camb)*, **2015**, doi:10.1039/c4ib00221k
- Wang, A. (2014) Nanoparticle formulations of siRNA: the next generation of targeted therapy for lymphomas and leukemias? *Ebiomedicine*, **2014**, doi:10.1016/j.ebiom.2014.11.013